MIT Open Access Articles

Switchable piezoelectric transduction in AlGaN/GaN MEMS resonators

SWITCHABLE PIEZOELECTRIC TRANSDUCTION IN ALGAN/GAN MEMS RESONATORS

Laura C. Popa and Dana Weinstein
HybridMEMS Group, Massachusetts Institute of Technology, Cambridge, MA, USA

ABSTRACT

This work presents a new switching mechanism in piezoelectric transduction of AlGaN/GaN bulk acoustic resonators. A piezoelectric transducer is formed in the AlGaN, between a top Schottky electrode and a 2D electron gas (2DEG) as a second electrode. In the off state, this 2DEG can be depleted by applying a negative bias to the top electrode, suppressing transduction and reducing capacitive loading. Switchable AlGaN/GaN resonators are demonstrated from 240MHz to 3.5GHz with frequency-quality factor products up to 1.7×10^{12} in air. Switching is shown in both devices with passive piezoelectric and HEMT sensing, with >19dB suppression in the off state.

KEYWORDS

MEMS resonators, GaN, piezoelectric transducer, HEMT, Resonant Body Transistor

INTRODUCTION

The demand for broad-band configurable RF systems with excellent frequency selectivity is a growing priority for opportunistic use of the over-crowded radio spectrum. High-Q MEMS resonators, with small footprint and monolithic integration, can provide RF building blocks for such spread-spectrum ad-hoc radios.

While high-Q MEMS resonators provide narrow bandwidth selectivity, broad-band operation typically requires a large bank of switchable devices. This bank introduces a large capacitive load at the input due to the drive transducers. Typically, piezoelectric resonators have strong coupling coefficients between electrical and mechanical domains enabling low loss filters. However, they must be switched in line of the RF signal, resulting in insertion loss and reduced power handling in configurable systems. This work presents a new implementation of piezoelectric transduction in an AlGaN/GaN heterostructure which enables on/off switching of piezoelectric transduction with DC voltage applied out-of-line of the RF signal, and reduces the capacitive load of the resonator by >10× when in the off state.

Gallium Nitride (GaN) based devices exhibit high piezoelectric coefficients (k_T^2 up to 2%) and excellent mechanical properties. GaN technology also provides high electron velocities, charge densities (1×10^{13} cm^{-2} in AlGaN/GaN), and critical electric fields (>3 MV/cm), ideal for high power (>10W/mm), high frequency (>100 GHz) ICs. This technology enables the integration of high-Q MEMS resonators with millimeter-wave ICs (MMICs) and high power electronics.

2DEG TRANSDUCTION

The switchable piezoelectric transducer presented in this work implements a 2DEG electrode as one of two electrodes needed to drive acoustic waves in a resonant AlGaN/GaN stack [1]. 2DEG electrodes have previously
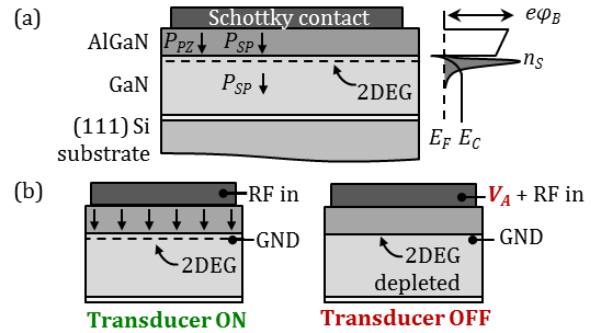

Fig. 1: (a) 2DEG confined in conduction band potential well at the interface between AlGaN and GaN. (b) Principle of switchable piezoelectric transduction.

been demonstrated as interdigitated transducers in a SAW AlGaN/GaN filter [2] as well as for piezoelectric actuation of AlGaN/GaN heterostructures [3].

The starting AlGaN/GaN heterostructure used in this work is illustrated in Fig. 1(a). Large spontaneous and piezoelectric polarizations form a sharp potential well confining electrons in a 2D plane just below the interface of AlGaN and GaN [4]. Typical electron densities of the resulting 2DEG can be as high as $n_S \sim 1\times10^{13}$ cm^{-2} and the mobility can reach 1500 cm^2/Vs, which makes the 2DEG conductive enough to serve as an electrode for piezoelectric transduction.

To drive acoustic waves in the structure, an AC electric field is applied across the AlGaN, between the 2DEG electrode and a Schottky metal contact (Fig. 1(b)). By applying a negative bias voltage to the metal electrode above the AlGaN, the 2DEG can be depleted away. This is the same principle used to switch the conduction channel in AlGaN/GaN High Electron Mobility Transistors (HEMTs). When implemented in an acoustic resonator, the removal of this bottom electrode suppresses electromechanical transduction and serves to reduce the capacitance of the drive transducer by >10×.

SWITCHABLE RESONATORS IN GAN MMIC TECHNOLOGY

The ability to switch piezoelectric transduction relies on the presence of a 2DEG, which is a feature of existing MMIC technology. This technology can be leveraged to fabricate passive and active (HEMT-sensed) switchable piezoelectric resonators with only two additional masks as shown in Fig. 2. The starting material is an AlGaN(25nm)/GaN(1.7µm) stack grown by Molecular Beam Epitaxy on a (111) Silicon substrate, using a thin AlN nucleation layer [5]. The growth for the devices in this work was performed at Raytheon with subsequent fabrication at MIT. Electrical isolation between different 2DEG regions (e.g. drive and sense) is realized through a BCl$_3$/Cl$_2$ plasma etch of the AlGaN. The 2DEG is removed from the regions where the AlGaN is etched
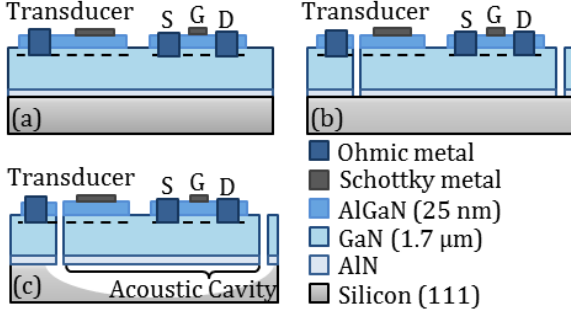
Fig. 2: Fabrication involves two additional steps to (a) existing GaN MMIC technology, including (b) a deep GaN etch, and (c) a release step.

Fig. 3: SEM of passive resonator, a 7.3×70µm bar with symmetric electrode configuration for drive and sense.

away. A Ti/Al/Ni/Au metal stack is deposited and patterned, followed by a rapid thermal anneal (RTA at 870°C, 30 sec) to form Ohmic contacts to the 2DEG. Atomic layer deposition of a 17 nm Al_2O_3 layer is used as a gate dielectric to minimize gate leakage. A Ni/Au/Ni gate metal stack is then deposited and patterned, followed by a 30 sec RTA at 500°C, to form Schottky electrodes. At this stage, both the piezoelectric transducer and the HEMT are formed (Fig. 2(a)). An additional Cl_2 ICP etch of the GaN layer defines the acoustic cavity (Fig. 2(b)). Electrical routing for both 2DEG and Schottky electrodes is achieved through routing beams. Finally, a XeF_2 isotropic Si etch releases the resonators from the substrate (Fig. 2(c)).

PASSIVE PIEZOELECTRIC SENSING

Passive 2-port piezoelectric AlGaN/GaN resonators were realized in this technology, driven and sensed using the 2DEG transduction mechanism described above. One such device is shown in Fig. 3 with symmetric drive and sense transducers.

When driven at acoustic resonance, strain fields defined by the mode shape induce a polarization field through the direct piezoelectric effect. For Wurtzite crystal materials such as GaN, the induced polarization field can be written as:

$$\boldsymbol{P_{PE}} = (e_{51}\epsilon_{zx})\hat{\boldsymbol{x}} + (e_{51}\epsilon_{yz})\hat{\boldsymbol{y}} + \left(e_{31}\epsilon_x + e_{31}\epsilon_y + e_{33}\epsilon_z\right)\hat{\boldsymbol{z}} \qquad (1)$$

Taking z along the Wurtzite c-axis, ϵ_x, ϵ_y, and ϵ_z are the strains along the x, y and z-axis respectively and ϵ_{yz} and ϵ_{zx} are shear strains. Here, e_{31}, e_{33} and e_{51} are the piezoelectric coefficients found in the Wurtzite crystal structure. There are two contributions to the bound charges associated with this polarization field. First, an interface charge σ is generated by a discontinuity in the polarization at the AlGaN/GaN interface, induced by the difference in piezoelectric coefficients of the two materials:

$$\sigma = (\boldsymbol{P_{PE,AlGaN}} - \boldsymbol{P_{PE,GaN}}) \cdot \hat{\boldsymbol{z}} \qquad (2)$$

Second, the polarization generates volume charge ρ throughout the heterostructure:
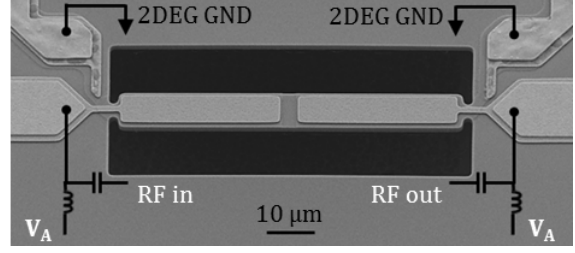
$$\rho = -\nabla \cdot \boldsymbol{P_{PE}} \qquad (3)$$

This mechanically induced charge is compensated by free charge flowing into the 2DEG, and can be measured as an AC current flowing into the top metal electrode.

The measured frequency response of the 2-port piezoelectric resonator shown in Fig. 3 is presented in Fig. 4. This device was measured in air in an RF probe station, and de-embedded using an open structure fabricated on the same chip. Two bending modes are detected at 243 MHz and 246 MHz, with Q's of 608 and 910, respectively. The insets in Fig. 4 show COMSOL simulations of the displacement fields of these resonant modes. Applying $V_A = -7$ V to the drive transducer depletes the 2DEG and suppresses the resonance signal by more than 19 dB. This also serves to reduce the drive capacitance C_0 by 13×, in close agreement with experimental measurements on AlGaN/GaN Schottky diodes [6]. For this measurement, the sense transducer remains on to demonstrate the effect of drive suppression alone, but can also be switched off for better isolation.

The small signal equivalent circuit of this resonator is shown in Fig. 5. The mechanical domain can be modeled by two RLC branches in parallel, corresponding to the symmetric and antisymmetric mechanical modes. The extracted drive capacitance C_0 and the lumped resistance of the 2DEG electrode R_{2DEG} are 390 fF and 3.8 kΩ, respectively. Fitting measured data to the full small signal model in Fig. 5, R_m of 117.5 kΩ and mechanical Q of 650 are extracted for the symmetric mode, and R_m of 71.3 kΩ and Q of 940 for the asymmetric mode.

There are two main contributions to the feed-through signal, including a capacitive contribution of the fringing electrical fields through the substrate, C_{ft}, and a
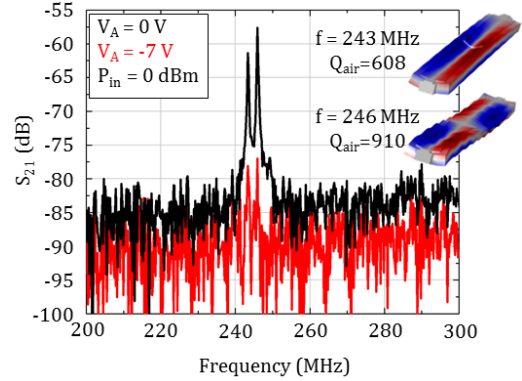

Fig. 4: Measured frequency response of passive resonator in air, showing 19 dB suppression of the signal when transducer is switched off ($V_A = -7$ V).
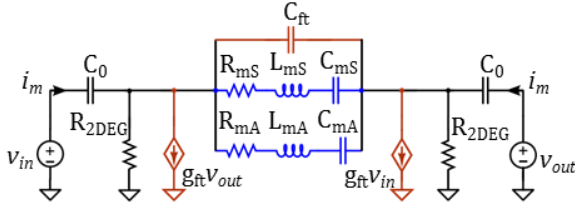
Fig. 5: Small signal equivalent circuit of the passive piezoelectric AlGaN/GaN resonator.

transconductance, g_{ft}. This second contribution can be understood as a modulation of the 2DEG at one port due to a signal applied at the other port. When resonators are scaled for multi-GHz operation, the out-of-band rejection of the transmitted signal is compromised by the increased feed-through floor.

ACTIVE HEMT SENSING

To achieve high frequencies of operation in MEMS resonators we have previously shown the benefits of active sensing using transistors embedded in the resonant structure [7]. This can be implemented in AlGaN/GaN devices by taking advantage of HEMTs inherent to this technology. The HEMT provides electromechanical amplification of the mechanical signal prior to external parasitics, enabling sensing at much higher frequencies than possible with passive devices. As shown in Fig. 2, the fabrication of these resonators involves only two additional steps to a standard GaN HEMT technology, which allows for both monolithic integration with MMICs and the ability to use HEMTs embedded in resonators as active sense transducers. Though both platforms have been previously demonstrated [8,9], this work presents the first use of a HEMT for active pick-off in a bulk acoustic AlGaN/GaN resonator to achieve multi-GHz frequencies.

As in the case of the passive resonator, strain fields couple piezoelectrically into an induced polarization. At resonance, this polarization induces an AC modulation of the 2DEG sheet density in the channel of the HEMT, through the charge contributions discussed in Eqs. (2) and (3). This charge modulation translates into an AC modulation of the drain current. Fig. 6 illustrates the equivalent small signal model of the actively sensed device. In the electrical domain, this device can be decomposed into two branches. The RLC branch corresponds to the mechanical resonance, and is equivalent to a 1-port passive device. The second branch is a modified HEMT small signal model. Here, g_α is an electromechanical transconductance dependent on the piezoelectric properties of the devices, while the parasitic feed-through includes a broadband transconductance, g_{ft}, a capacitance, C_{ft}, and a substrate resistance r_{ft}.

DC Performance of HEMT-Sensed Resonator

An SEM of a piezoelectric AlGaN/GaN resonator with an embedded HEMT for active sensing is shown in Fig. 7. Though regions of the Ohmic contact are consumed during the high temperature anneal, conductive paths are continuous along the length of the source and drain regions of the HEMT.

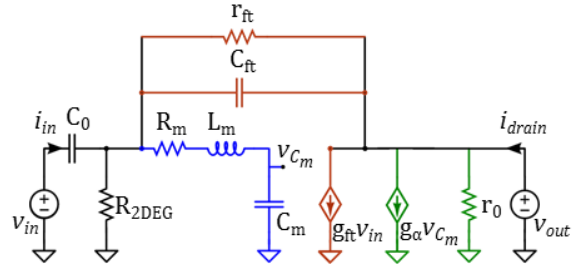Fig. 8 shows the measured DC behavior of the HEMT

Fig. 6: Small signal equivalent circuit of the piezoelectric drive HEMT-sensed AlGaN/GaN resonator.

embedded in the resonant structure (a) before and (b) after the XeF₂ release step. Prior to the release step, the HEMT has a threshold voltage $V_T = -6.2$ V, which corresponds to a 2DEG density of 5×10^{12} cm^{-2}. After release, the HEMT exhibits $V_T = -5.75$ V, and the extracted charge density drops to 4.6×10^{12} cm^{-2}. One possible reason for this current reduction is the generation of surface defect states during the final fabrication steps, with a direct impact on the electron density in the 2DEG. These surface effects can be alleviated by introducing a passivation layer early in the process [10]. Another possible cause of this degradation is the stress relaxation due to the release of the structure [11]. Using an optical profilometer to measure the radius of curvature of the released resonators, an initial compressive stress of 1.4 GPa was found at the GaN/Si interface.

In addition, a 2× reduction in the drain current in the saturation regime is observed, caused by the high channel temperature. AlGaN/GaN HEMTs on Silicon substrates have been shown to exhibit channel temperatures as high as 350°C [12]. After the release step, the HEMT is thermally isolated, increasing the operational temperature. This reduces the mobility of the 2DEG, which translates into an increase in the channel resistance and a negative differential resistance at the output of the HEMT, as
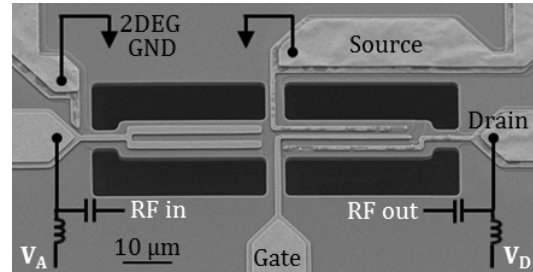

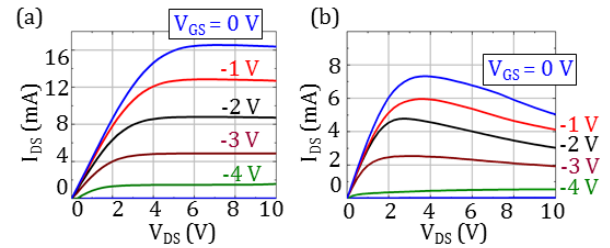*Fig. 7: SEM of piezoelectric-drive, HEMT-sensed 8.7×70μm resonator. The HEMT has gate length of 1 μm.*

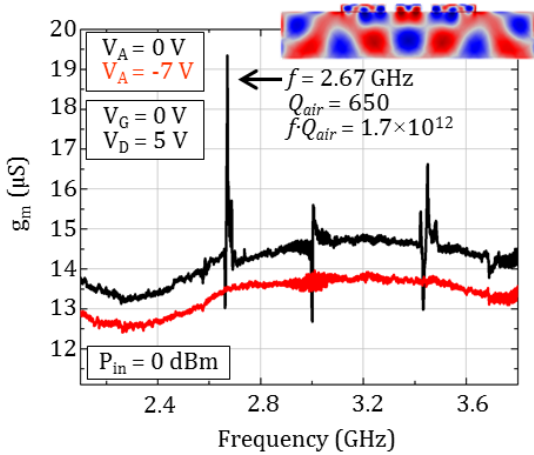*Fig. 8: Measured IV curves of the HEMT embedded in resonator (a) before and (b) after release step.*

Fig. 9: Measured frequency response of PE drive-HEMT sense AlGaN/GaN resonator, in air. The transconductance, $g_m = Y_{21} - Y_{12}$, is suppressed when the 2DEG under the drive electrode is depleted.

observed in Fig. 9(b). Both stress and temperature effects can be alleviated through an increased number of suspension beams of the resonator, which has also been shown to suppress spurious modes and enhance Q [13].

RF Performance of HEMT-Sensed Resonator

Using HEMT sensing, resonators up to 3.5 GHz were realized and detected with simple 2-port measurements as shown in Fig. 9. The active device is measured in air with 50Ω termination. While a Line-Reflect-Match algorithm was used to de-embed the testing setup up to the RF probes, no on-chip de-embedding structures were used. The resonance at 2.67 GHz has Q of 650 in air with $f \cdot Q$ of 1.7×10^{12}, the highest reported in GaN resonators to date. A COMSOL simulation of the stress distribution of this resonance is shown as an inset in Fig. 9, with maximum stress under the gate of the transistor. This translates into an efficient modulation of the charge density in the channel of the HEMT. As in the case of the passive device, applying a negative bias $V_A = -7$ V to the drive transducer depletes the 2DEG and suppresses the resonance signal, while reducing the drive capacitance C_0 by 13×.

CONCLUSION

A switchable piezoelectric transducer implemented in an AlGaN/GaN heterostructure is introduced and demonstrated on the drive of passive and active MEMS resonators up to 3.5 GHz. This switchable transducer reduces capacitive loading by an order of magnitude when the resonator is not in use, providing a building block for configurable RF filtering in existing MMIC technology. For additional isolation, the sense transducer of these 2-port devices can also be switched. In the case of the passive resonator, this can be achieved by the same principle of 2DEG depletion. In the HEMT-sensed device, $I_{on}/I_{off} > 10^6$ can be leveraged for off-state isolation. This work is also the first to use a HEMT for active electromechanical detection in bulk acoustic AlGaN/GaN resonators at multi-GHz frequencies, resulting in the highest reported $f \cdot Q$ product in GaN.

REFERENCES

[1] K. Brueckner et. al., "Two-dimensional electron gas based actuation of piezoelectric AlGaN/GaN microelectromechanical resonators", *Appl. Phys. Lett.,* vol. 93, 173504 (2008).

[2] K.-Y. Wong et. al., "Surface acoustic wave device on AlGaN/GaN heterostructure using two-dimensional electron gas interdigitated transducers", *Appl. Phys. Lett.,* vol. 90, 213506 (2007).

[3] K. Tonisch et. al., "Piezoelectric actuation of (GaN)/AlGaN/GaN heterostructures", *J. Appl. Phys.,* vol. 104, 084516 (2008).

[4] O. Ambacher et. al*.,* "Two-dimensional electron gases induced by spontaneous and piezoelectric polarization charges in N- and Ga-face AlGaN/GaN heterostructures", *J. Appl. Phys.,* vol. 85**,** 6 (1999).

[5] T.E. Kazior et. al., "High Performance Mixed Signal and RF Circuits Enabled by the Direct Monolithic Heterogeneous Integration of GaN HEMTs and Si CMOS on a Silicon Substrate", *CSICS,* 1-4, (2011).

[6] Y. Lv et. al., "Extraction of AlGaN/GaN heterostructure Schottky diode barrier heights from forward current-voltage characteristics", *J. Appl. Phys., vol.* 109**,** 074512 (2011).

[7] D. Weinstein et. al., "The Resonant Body Transistor" *Nano Lett.,* vol. 10(4), 1234-37 (2010).

[8] M. Faucher et. al., "Amplified piezoelectric transduction of nanoscale motion in gallium nitride electromechanical resonators", *Appl. Phys. Lett.,*vol. 94, 233506 (2009).

[9] A. Ansari et. al., "Monolithic Integration of GaN-Based Micromechanical Resonators and HEMTs for Timing Applications", *IEDM,* 363-6 (2012).

[10] B.M. Green et. al., "The Effect of Surface Passivation on the Microwave Characteristics of Undoped AlGaN/GaN HEMTs", *Electr. Dev. Lett.*, vol. 21, 268-70 (2000).

[11] M. Azize et. al., "Effect of substrate-induced strain in the transport properties of AlGaN/GaN heterostructures", *J. Appl. Phys.,* vol. 108, 023707 (2010).

[12] J. Kuzmik et. al., "Determination of Channel Temperature in AlGaN/GaN HEMTs Grown on Sapphire and Silicon Substrates Using DC Characterization Method", *Trans. Elec. Dev.*, vol. 49, 1496-98 (2002).

[13] B.P. Harrington et. al., "Toward ultimate performance in GHz MEMS resonators: Low impedance and high Q", *MEMS*, 707-10 (2010).

CONTACT

*L.C. Popa, tel: +1-617-452-2861; lpopa@mit.edu